ORIGINAL ARTICLE

CrossMark

A method for mechanical property assessment across butt fusion welded polyethylene pipes

Slimane Niou [1] · Kamel Chaoui [1] · Salaheddine Azzouz [2] · Nacira Hamlaoui [3] · Latifa Alimi [4]

Abstract

The use of high-density polyethylene pipes in gas and water distribution networks is steadily growing worldwide. If the resistance of plain pipes is at present time well established using appropriately designed standards, welding issues continue to be globally approached equally in terms of structure and mechanical properties. Consequently, further practical investigations should be aimed at studying mechanical properties in the weld region which includes the melt zone and its heat-affected zones. This work presents a method based on removing layers in order to assess localized variances in mechanical properties throughout the weld seam in both radial and circumferential directions. An experimental plan based on specific machining operations allowed testing 39 standard specimens representing the weld volume matter in three concentric layers for given pipe dimensions and their counterpart standard unwelded ones. The typical stress–strain behavior of semi-crystalline materials is preserved in welded and unwelded specimens but with different characteristic limits. At the weld inner layers, properties such as elastic modulus, yield, and failure stresses displayed lower values, whereas in welded outer layers, the tendency is inversed. The cold drawing extend remained approximately steady for unwelded and welded cases across the pipe wall. This property is less affected by the presence of the weld as it described a constant material flow which is mostly a function of available material quantity for yielding. The approach developed in this study gives consistent indications on welding quality around the pipe weld and across the thickness. Accordingly, outermost and innermost welded layers may exhibit lower or even bad-quality welds as imperfections can concentrate stresses at the joint interface because of cold weld problems. Such method enabled detecting 23% of failures at the weld seam from outer and inner layers while the middle layer did not reveal any failure at the weld. The causes of this behavior are approached using crystallinity evolution in welded and unwelded pipes.

Keywords HDPE pipe · Butt fusion welding · Mechanical properties · Radial direction · Circumferential direction · Structural variances

✉ Kamel Chaoui
chaoui.kam23@gmail.com; kamel.chaoui@univ–annaba.dz

1 Mechanics of Materials and Plant Maintenance Research Laboratory (LR3MI), Mechanical Engineering Department, Faculty of Engineering, Badji Mokhtar University of Annaba (UBMA), PO Box 12, 23052 Annaba, Algeria

2 LR3MI, Ecole Supérieure des Technologies Industrielles (ESTI), Cité Safsaf, PO Box 218, 23012 Annaba, Algeria

3 LR3MI, Mechanical Engineering Department, Faculty of Sciences and Technology, 8 May 1945 University of Guelma, PO Box 401, 24054 Guelma, Algeria

4 LR3MI, Centre de Recherche en Technologies Industrielles (CRTI), Route de Dély-Brahim, PO Box 64, 16014 Chéraga, Algiers, Algeria

1 Introduction

High-density polyethylene (HDPE) pipes continue to be the focus of interesting and innovative studies in relation essentially to manufacturing processes, structure–property relationships, and novel applicative developments [1–4]. For instance, many recent studies and reviews dealt with testing techniques [5, 6], toughness evaluation [7], welding methods [8], aging phenomena [9], machining operations [10, 11], and safety appraisal [12, 13].

The issue of differences in mechanical properties through the wall of extruded parts under specific conditions has been explained in terms of structural variances (morphology) and residual (internal) stresses [14–17]. In the case of extruded pipes made from high-density polyethylene resins, the problem was approached experimentally in two phases as it was

necessary to solve difficulties related to the nature of the method to be adopted in order to extract the most wanted properties (destructive or non-destructive). In the literature, non-destructive methods are used to characterize only thin layers out of the pipe wall. However, to achieve a whole idea on property distribution and heterogeneities in thick pipes (thickness ≥ 10 mm), we need to use machining techniques at adequate operating conditions which should minimize both material deformations and frictional heat generation in order to avoid needless structural changes [10, 11, 16, 18, 19].

In a primary phase, HDPE long filaments were orthogonally machined under specific conditions in order to illustrate the entire thermal and structural history rooted in the pipe wall because of manufacturing process (i.e., one filament extends from the outside pipe surface to the inside). It has been shown that a distribution of mechanical properties existed and was correlated with pipe wall morphology using crystallinity [16, 20, 21]. These correlations were also found to be affected by the presence of aggressive media such as acids, crude oil, and other oxidizing environments [20]. In a second phase, following several reviewers' recommendations, the machining parameters were improved to produce standardized test specimens according to ASTM representing different layers across the pipe wall (i.e., in the longitudinal direction). As usual, the lowest possible level of deformations, the least heat generation (or lowest cutting zone temperature), and the minimum surface roughness were sought to keep to a minimum structural disturbances within the material [10, 11]. It was observed that stress-related properties increased from outer towards inner layers implying an important effect of morphology particularly crystallinity and absorbed liquids [22, 23].

When standard specimens were exposed to aggressive environments, it was found that mechanical properties for inner, intermediate, and outer layers followed similar degradation trend: Toluene-methanol is the most aggressive followed by sulfuric acid and then comes distilled water. It was also found that both Young's modulus and yield stress are increasing from outer towards inner pipe layers in all testing environments. Such progression was essentially attributed to changes in crystallinity combined with embedded internal stresses due to the extrusion process and to the product geometry (cylinder) [22]. In a further study, it was noted that mechanical properties of inner layer are much better than those of outer one. The plastic hardening is important at the outer surface most probably because of higher compressive residual stresses imparted by extrusion process [23].

Many investigations have been conducted on butt fusion welding (BFW) of polyethylene pipes under service conditions and at laboratory scale. The objectives varied from understanding the mechanisms of the welding process and associated phenomena responsible for the formation of the weld seam to numerical simulations coupling both thermal and mechanical effects. Further industrial and methodological topics are dealing with defect diagnosis and quality control methods

for welded pipes, such as defect detection by thermal IR imagery or ultrasonic-phased array inspection [24, 25]. In addition, typical studies include mechanical characterization of the weld joint [8, 14, 17], thermal studies [26, 27], and rupture/failure phenomena [3, 28, 29]. An exhaustive study on butt welding was performed to compare experimental and numerical results in terms of temperature distributions, tube displacements under the effect of welding pressure, and the dimensions of the created weld beads. The results are rather reasonable since the simulations lead to weld beads whose shapes are close to those experimentally obtained. Moreover, temperature evolutions at various welding stages are comparable to the measurements made via implanted thermocouples. Simulated pipe displacements during welding stages are also alike to measured ones in terms of direction of variation, although the orders of quantities are different [27].

In the same tendency, a reasonable extension of the already-achieved investigations [16, 20–23], a new research should be devoted to ascertain the distribution of mechanical properties in butt welds. This study must necessarily treat two aspects: (i) the evolution of mechanical properties at the weld seam, i.e., across the pipe wall (or radial direction) and (ii) the variances of mechanical properties around the pipe boundary (or circumferential direction). The experimental investigation of these points should improve our understanding of both weld-localized resistance and failure aspects in view of existing standards [30–33].

The aim of this research is to establish and experiment a method based on machining in order to obtain localized mechanical properties in butt fusion welds of polyethylene pipes. In this work, the five steps of the method have been implemented and the results are discussed in terms of mechanical property variances between welded and unwelded material using stress–strain behaviors. In addition, the method is used to scrutinize the whole weld interface seeking probable weak areas and to establish a relationship with the unwelded matching counterparts.

2 Presentation of the method

Butt fusion welding of HDPE pipes is a common welding technique which is performed in four successive steps while controlling both time intervals and applied pressures (Fig. 1). The welding surfaces are prepared according to approved standard procedures to ensure a final proper joining of two pipe segments [30–33]. Usually, these parameters are provided by manufacturers on a magnetic card for each pipe lot (pipe resin, OD, t, and SDR) to make sure that corresponding welding input data are exact and the operation is performed at the optimal conditions in the field. The heating up to melting of polyethylene material is achieved using a hot metallic plate under a precise pressure developed by a mechanical

Fig. 1 **a** Diagram illustrating the four steps of a butt fusion welding (BFW) procedure. **b** Welded HDPE pipe segments (in the field)
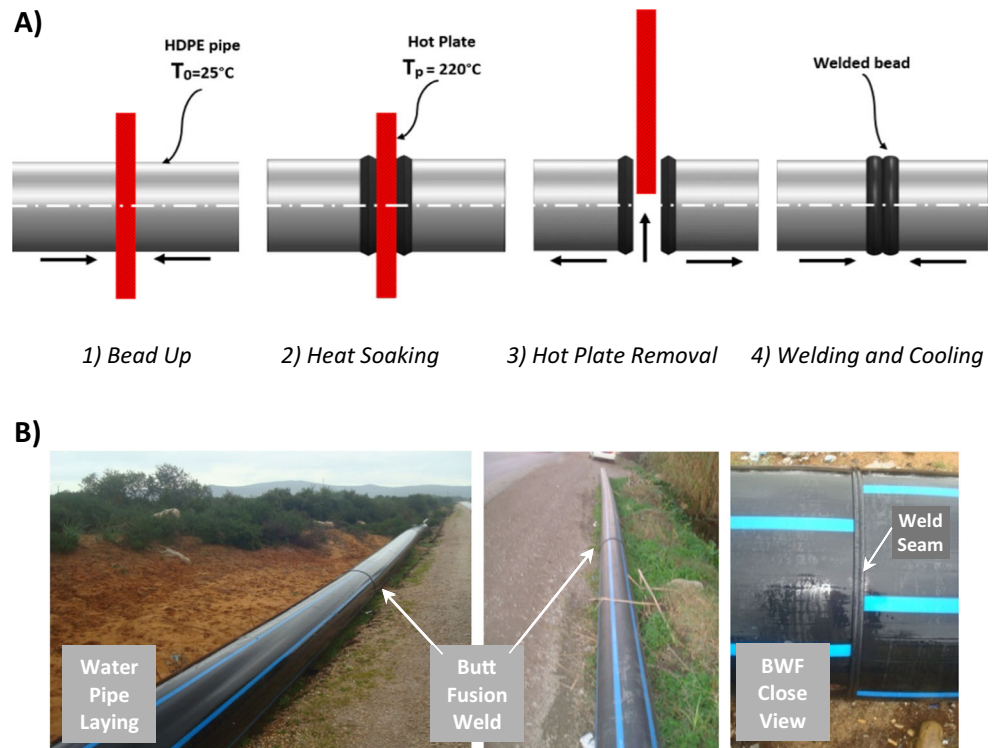

apparatus which firmly holds both pipe segments. In the heat soaking step, heating is kept on; however, the applied pressure is reduced to allow melted material to grow up in depth. Once the melting time is reached, the hot plate is removed in a very short time to trim down heat losses and the melted pipe ends are brought together rapidly. Finally, a specified pressure is applied allowing the weld to shape up and the melt to flow outward forming a curling. At the molten interface, polymer chains are supposed to entangle with each other, and subsequently, progressive cooling and solidification take place at ambient temperature [14, 27, 28].

Most probably, the main reason leading to suggest this method is based on the analyses showing the contour of a butt fusion weld (BFW) as it appears from a longitudinal pipe cut as indicated in Fig. 2 [14, 28, 29]. The weld shape is characteristic for this joining technique, and it can be deduced that properties across pipe thickness are not homogeneous since the melt zone does not have a homogeneous interface, i.e., it is squeezed and reduced at the center and expanded at the borders (inner and outer surfaces). In order to investigate such heterogeneity in pipe structure–property relationship, it is mandatory to explore how to get to localized properties inside the pipe wall. To fulfill the standard requirements for mechanical testing, appropriate dimensions should be met. Figure 3 summarizes available standard dimensions for mechanical strength tests under tension and indicates that type IV specimen is the only solution to extract three contiguous layers from the given wall thickness that meet the requirements. The proposal is to manufacture specimens which allow

obtaining properties at various depths across the thickness within the pipe wall as presented in both Figs. 2 and 3.

The proposed method is a function of several factors which may restrict the accessibility to different properties in the welding zone. In fact, confined mechanical and structural properties of the weld are not easily accessible by practical and sensible non-destructive techniques as it is for conductive metallic materials. Previously, a method with a similar object has been anticipated, and it allowed the interpretation of some property variances across pipe wall; however, the tested pipe specimens were unwelded, and the results were obtained using a non-standardized process based on filament machining [16, 20]. Another important limitation for current
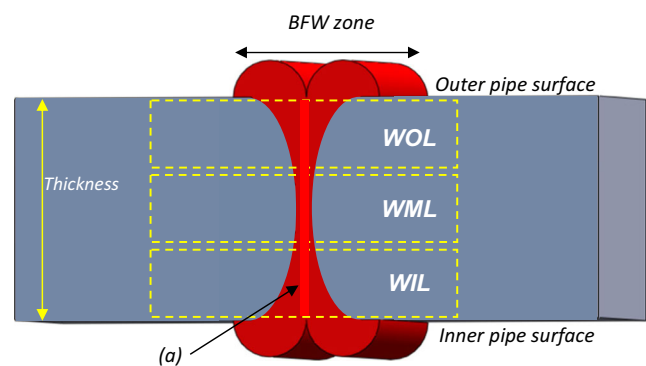
Fig. 2 Contour of a butt fusion weld (BFW) as it appears from a longitudinal pipe cut and boundaries of the three contiguous layers where welded specimens are extracted (WOL, WML, WIL). Arrow (a) indicates the mid-plane of the weld where crystallinity is the highest [14, 29, 34]
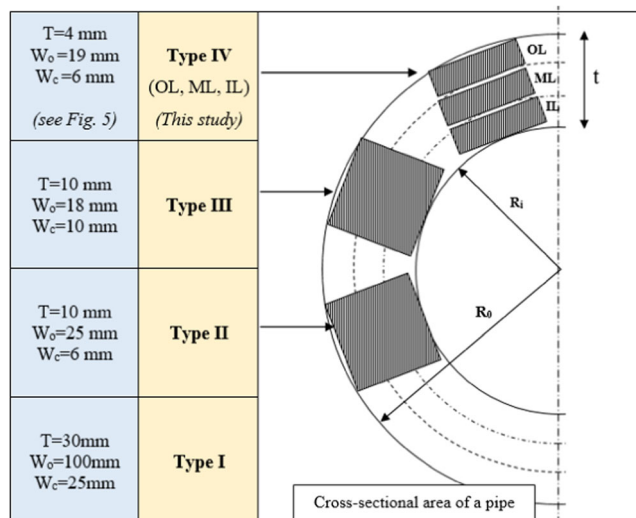
Fig. 3 Standard test specimen type IV as a solution for manufacturing three identical side-by-side specimens (IL, ML, and OL) from the pipe wall thickness. (Right illustration is a cross-sectional pipe cut)

standards is testing pipe specimens with important thicknesses and high outside diameters (OD) [30]. For instance, the minimum thickness of a 2000-mm OD pipe should not be less than 48.8 mm which is far away from the 4 mm requested for a type IV specimen [31]. Although it is accepted for unwelded cases, but once the tested material contains a butt fusion weld, the global approach ultimately will hide from view observations that are needed for weld performance assessment. Finally, current standards do not mention any hint on the location of the tested specimen since it is assumed that measured properties are independent of radial positions.

The present method becomes interesting as it provides alternatives to the previous limitations; i.e., obtaining an idea about local properties within the weld at many positions along the circumference and for three radial layers. By combining machining processes, these layers were obtained in the form of three concentric cylinders from the same tube provided that not to lose any material at the interfaces [21, 22]. Figure 4 presents the five steps of the manufacturing processes developed to achieve such goals. The details of each phase of the proposed method are illustrated in Table 1 together with the different technical conditions and the appropriate standards which guided parameter selection. In this case, the method requires working on HDPE pipes that allow obtaining at least three contiguous standard type IV specimens from the wall as indicated in Fig. 3. In fact, such condition is governed by the standard dimension ratio (SDR) parameter which is defined for plastic pipe manufacturing by the following relationship:

$$SDR = \frac{OD}{t_{min}} \qquad (1)$$

with OD the outside diameter (mm) and t_{min} the minimum thickness (mm). The standardized HDPE outside

diameters range from 16 to 2000 mm, which allows corresponding SDR values to vary from 6 to 41 [31]. In *phase 1* pipe dimension selection is decisive as SDR is the criterion of choice based on the minimum thickness that meets the prescribed condition (Fig. 1). In fact, a minimum of three specimens is essential to build a trend in the radial direction since non-uniformity effects on weld resistance might not be severe along the circumference as compared to the radial direction where crack initiation and propagation are the most probable to happen. Therefore, the plan is to discern at least three contiguous surface areas (Fig. 3) that are designated in this study by WOL, WML, and WIL (Fig. 2) as indicated in *phases 2 and 3* (Fig. 4 and Table 1). It should be emphasized that machining conditions are very critical for such studies because a choice of injudicious cutting parameters will indeed influence measured results. Therefore, adapted cutting regime is supposed to prevent higher material deformation and should lower heat generation in order to preserve the original structure [10, 11].

At the end of *phase 3*, properly identified HDPE samples (θ and r) may be taken for structural or other characterizations such as crystallinity or microindentation measurements [14, 21, 28, 29]. Then, once the dimensions are adequate, the extraction of the standard test specimens is started simultaneously with codification and conditioning as illustrated in *phase 4*. It should be noted that these operations are carried out at the same time for welded and unwelded specimens. Finally, in *phase 5*, the mechanical tests are performed according to the standards and following the provided protocols of the method (Table 2).

3 Experimental approach

3.1 Material

The material used in this study is a high-density polyethylene (HDPE-100) water pipe. Its maximum service pressure is 10 bars (PN 10), and it was manufactured by the Algerian plastic pipe company STPM CHIALI, Sidi Bel-Abbès, Algeria [32]. It is extruded according to the standards EN 12201 (Parts 1–7) and ISO 4427 (Parts 1–4) which correspond to the Algerian Norm NA 7700 [32]. The pipe outside diameter (OD) is 200 mm, and its average wall thickness is 11.9 mm (SDR = 17). Table 3 summarizes some mechanical properties in the solid state and at ambient temperature.

3.2 Butt fusion welding

The experimental work consisted in preparing, from the same pipe section, three butt fusion joints following identical cutting, edge preparation, and welding conditions
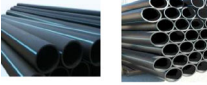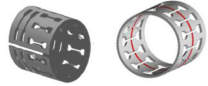
Fig. 4 Flow chart of process method and its manufacturing phases
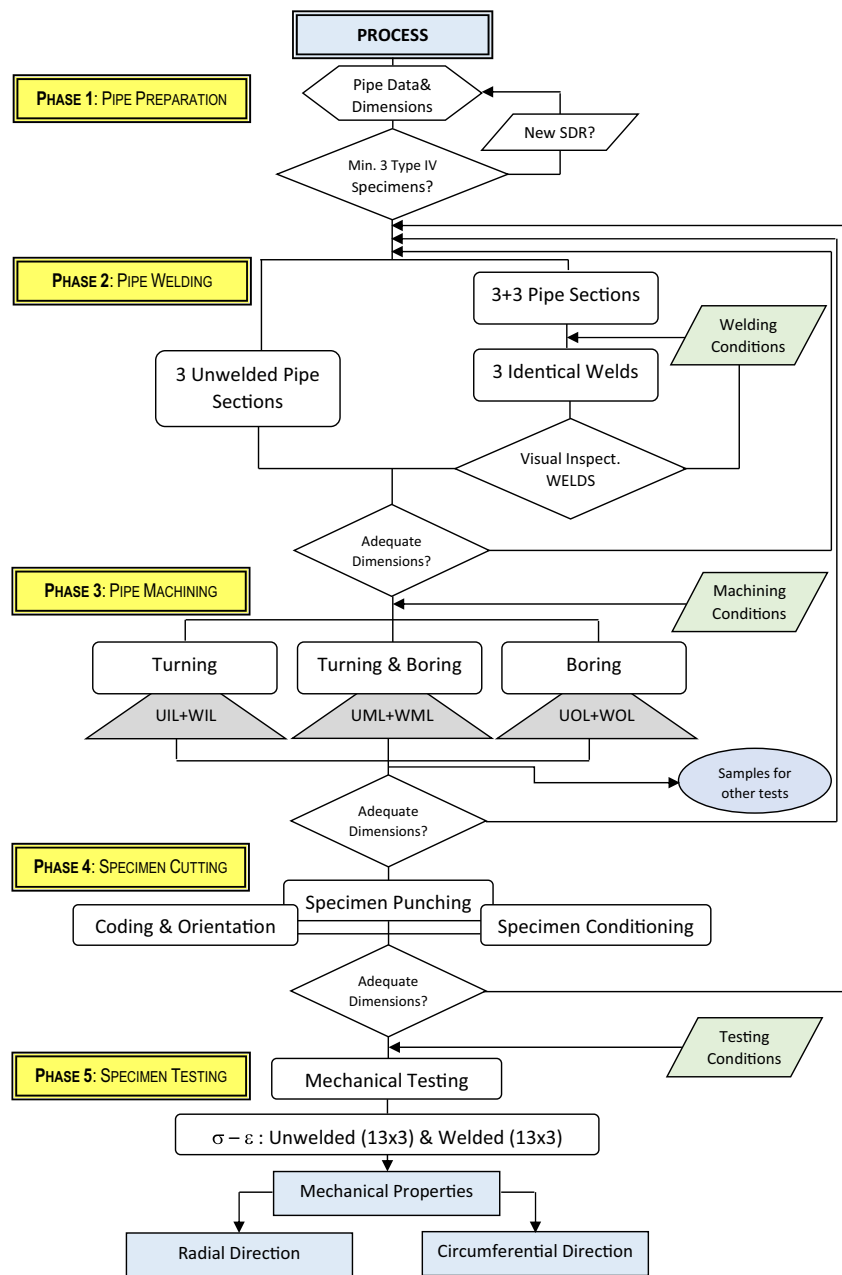
(Fig. 1). The pipe cutting and welds are performed in a row to keep original pipe orientation as it was manufactured and to minimize any induced damages due to handling operations. The welding operations were carried out in the field using the BARBARA-J. SAURON PilotFuse Unit, Type PL-315 according to ISO-12176-3 [33]. The welding machine is able to perform pipe welds on diameters ranging from 160 to 355 mm. It develops a nominal power of 6 kVA when it is fed by 220 V. The work cycle is unrolled automatically according to the digitally input data of the pipe resin. It is noted that the operator intervenes only for the implementation of auxiliary tools (pipe surface planer and heating mirror) and for the visual control

operations (cleaning, alignment, and surface evenness). In general, three essential elements contribute to obtain an adequate weld: (i) cleanliness of joint surfaces, (ii) qualified technical training for the manipulator, and (iii) properly dimensioned, controlled, and maintained welding equipment according to the procedure [33, 35]. The parameters of the butt fusion welding phases which are equalization, heating, plate retraction, and welding cooling are shown in Table 2. In this study, a typical bead up time of 21 s is used while heat soak and dwell times were, respectively, maintained at 180 and 10s. The measured average weld seam widths and heights are, respectively, 18.32 ± 0.31 and 4.73 ± 0.28 mm for the outer layers (WOL).

Table 1   Manufacturing operations and technical conditions for the proposed method

PHASE	MANUFACTURING OPERATIONS	SPECIFIC OPERATIONS	PRODUCT DESIGN	TECHNICAL CONDITIONS	MAJOR STANDARDS	REFERENCES
1	**Pipe Sampling**	Extruded pipe lots		HDPE, OD; SDR; Specimen: Type IV; t_{min} : Nb. Specimens ≥3. *(Figs.2 and 3)*	• ASTM D-3035-03 • EN 12201 • NA 7700 (NA: Algerian Std.)	[30,32]
2	**Pipe Welding**	3 Butt Fusion Welds		*(Fig.1 and Tab.2)*	• ISO-12176-3 • ASTM D-2657-07 • ASTM D-3261-03	[33]
3	**Pipe Machining**	*(Previous Studies)* Filament specimens: Orthogonal Machining.		Specific cutting tool; Specific regime: V_c; a_p ; No feed rate (f); Cutting: Through pipe wall.	• No available standard	[16,20]
		Standard specimens: Turning + Boring		Specific : V_c; f; a_p; Adapted tool geometry. *(Tab. 4)*	• ISO 2818 (1994)	[10,11,22] [31,35]
4	**Specimen Punching**	Slit rings; Mechanical Press; Directions: θ, r, z.		t_{sp} ≤ 4mm; Type IV. *(Figs. 3, 6 and 7c)*	• ISO-527-1 • ASTM D-638	[21,22,36]
5	**Standard Specimen Testing**	Universal Testing Machines : Tension…		Testing speed (mm/min); Ambient temperature; Automatic Data Acquisition; *(Figs. 3, 6 and 7c)*		[23,28,34] [31,35,36]

3.3 Machining of welded and unwelded pipes

The machining of the HDPE pipe has been the subject of several research studies seeking the most adapted cutting conditions which improve surface roughness and, at the same time, reduce generated heat at the tool-work piece contact edge [10, 11, 36]. Material removal was achieved on a TOS TENCIN lathe, model SN 40 having 6.6 kW power on the spindle. The turning and boring operations were carried out with the optimal parameters published in [36] and which are as follows: V_c = 355 rpm, f = 0.56 mm/rev, and a_p = 1 mm. Two lots of pipe portions (three unwelded and three butt fusion welded pipe segments) are prepared accordingly in order to manufacture six pipe envelopes defined by the limit condition [31]:

$$t_{(post-machining)} ≤ 4 \text{ mm} \tag{2}$$

Details of envelope dimensions after machining are indicated in Table 4. The objective is to manufacture three pipe envelopes representing the unwelded cases for outer, middle, and inner layers designated as UOL, UML, and UIL and which are considered as references for mechanical properties. Similarly, the welded pipes are used to manufacture three equivalent envelopes containing a specified part of the entire weld as illustrated in Fig. 5 (radial direction). The latter are designated by WOL, WML, and WIL and have alike positions as UOL, UML, and UIL, respectively (Table 4). Since the machining operations require supporting the plastic pipe by rigid steel sleeves, outer and inner weld seams have been removed allowing firm handling in lathe jaws [36].

Table 2   Nominal parameters for butt welding phases used in this study

Parameter	Welding phases			
	Bead-up (Pipe pressed against hot plate)	Heat soak (Pressure reduction)	Hot plate removal (Dwell time)	Welding and cooling (Function of pipe dimensions)
Pressure (N/mm²)	0.18	< 0.01	–	0.18
Temperature (°C)	220	220	–	–
Time (s)	21	180	10	1265

Table 3 Properties of HDPE-100 pipe material

Property	Value	Standard
Density (kg/m^3)	949–961	ISO-1183
MFI (g/10 min)	0.2–0.5	ISO-527:2
Young's modulus (MPa)	>1100	
Failure stress (MPa)	>24	
Tensile strain at break (%)	>500	
Shore D-hardness at 20 °C	59	ISO-868
Carbon black content (%)	2.0–2.5	ISO-6964

3.4 Specimen preparation and testing conditions

In order to experimentally assess the mechanical properties throughout the pipe wall, the recommendations of ASTM D-638 standard are applied [31]. The normalized testing specimen geometry type IV is shown in Fig. 6. In this work, the condition imposed by Eq. (1) about thickness remains unchanged. The tensile tests are carried out in the longitudinal direction (and around the pipe) which is perpendicular to the weld plane. The weld joint must be exactly in the mid-span of all the welded specimens (3 × 13 specimens), i.e., at a distance equal to G/2 (Fig. 6). This condition is important because the test specimens are designed to evaluate the resistance of the joint which must be aligned vertically with the tensile testing machine jaws. Figure 7 illustrates the three welded envelopes (inner: WIL, middle: WML, and outer: WOL) and the positions of extracted test specimens by press punching.

The tests were carried out on a ZWICK-Z010 testing machine having a maximum load cell of 10 kN. All tests were conducted at laboratory ambient temperature and at constant loading speed of 100 mm/min which has already been used in other studies [16, 21, 37]. The testing operation and data acquisition were monitored by a computer system, and the results were processed via the TestXpert® Software Version 9.01.

Crystallinity measurements were carried out using a DSC apparatus Type TA Instruments according to ISO-11357 which is a specific standard for polymers. The heating rate was 5 °C/min, and the value of reference enthalpy considered is 293 J/g.

4 Results and discussion

4.1 Basic pipe stress–strain behavior

Figure 8 shows the stress–strain behavior of test specimens machined from the commercial pipe basic material. Generally, for the three unwelded cases (inner: UIL, middle: UML, and outer: UOL), the mechanical behavior is very similar. It shows the three typical zones of semi-crystalline polyethylene resins under tension loads: (I) an elastic region limited by $\varepsilon \sim 20\%$ and σ_y (or $\sigma_{\text{max-elastic}}$), (II) a drawing zone characterized by necking (or multiple necking) propagation up to $\varepsilon \sim 300\%$, and (III) the plastic hardening phenomenon usually associated with a rise of macromolecular chain orientation until ductile failure occurs beyond $\varepsilon \sim 450\%$ [16, 20, 35, 37]. Since the required results are approached through complex machining and mechanical testing, reproducibility of the stress–strain behaviors (Fig. 8a–c) was an important criterion in order to ensure test reproducibility in the best conditions.

Results indicate that the inner layers (UIL, Fig. 8a) are more resistant in terms of σ_y than the UOL layers (Fig. 8c). The dispersion between the different $(\sigma$–$\varepsilon)$ curves becomes apparent as the deformation increases until it becomes more pronounced beyond 200% strain. On the other hand, the case UOL presented the maximum of variations as plastic hardening starts taking place; this could be in relation with the structure which is commonly more amorphous and subject to

Table 4 Pipe dimensions after machining outer, middle, and inner layers for unwelded and welded cases

PIPE HDPE-100 (SDR 17.6)	Original pipe dimensions	Dimensions after machining					
		Outer layer (OL)		Middle layer (ML)		Inner layer (IL)	
		UOL (1)	WOL (2)	UML (3)	WML (4)	UIL (5)	WIL (6)
OD (mm)	200	200		192		184	
ID (mm)	176.2	192.2		184.2		176.2	
Mean radius (mm)	Based on OD	100		96		92	
Number of punched specimens (type IV)		13	13	13	13	13	13
$t_{\min}$ (mm)	11.9	3.98 ± 0.17	3.98 ± 0.15	3.91 ± 0.10	3.93 ± 0.15	3.87 ± 0.15	3.96 ± 0.11

$t_{\min}$ (sought after machining) 4 mm

U unwelded, W welded

Fig. 5 a Schematic of HDPE weld across the pipe wall. **b** Identification of (I) inner, (M) middle, and (O) outer welded layers: WIL, WML, and WOL
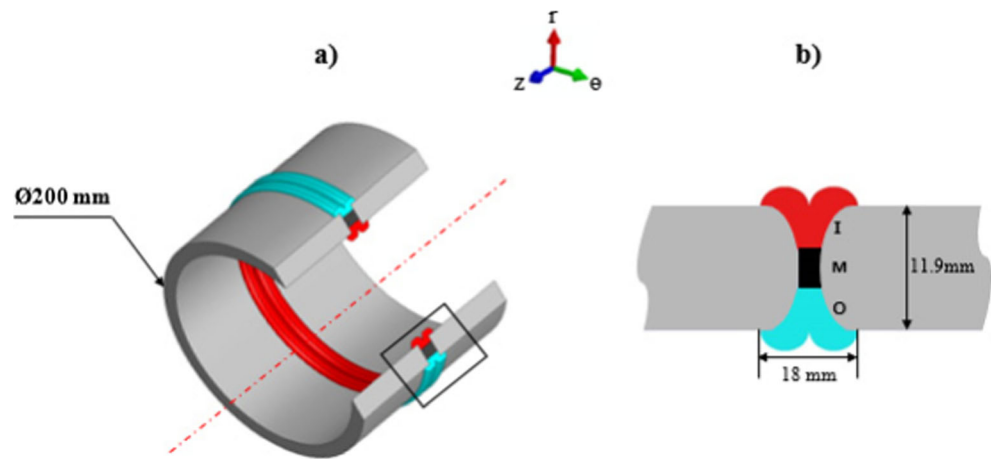

compressive internal stresses towards external pipe layers [21–23]. However, such dispersion at this position is less pronounced for UIL and UML cases (Fig. 8a, b) as the crystallinity usually increases when moving towards the innermost pipe layers. At the beginning of the plastic hardening stage ($\varepsilon \geq$ 325%), every curve for all layers (UIL, UML, and UOL) revealed a flatten portion (constant stress) within the strain interval 350 up to 400%, which is probably due to structural chain breaking down as a result of high stretching. For the average stress level of zone II (σ_{cd}), it is observed that the drawing is taking place with a decreasing stress from IL towards OL. The approximate upper and lower limit intervals for UIL, UML, and UOL are [16–18 MPa], [14–17.5 MPa], and [13–16 MPa], respectively (Fig. 8). Finally, it should be noted that the developed testing procedure allows illustrating a 2D synchronized representation of every single possible stress–strain curve for the unwelded cases (i.e., a total of 13 per layer, in this study) all along the pipe circumferential direction and at different positions in the radial direction (i.e., a total of 3).

4.2 Welded pipe stress–strain behavior

Figure 9 shows the stress–strain behavior of the three case studies (WIL: inner layer, WML: middle layer, and WOL: outer layer) once machined and prepared from butt welded pipes. Similarly, the three zones observed in Fig. 8 are maintained, but the limit values are quite different because of the welding joint incidence and the resulting effects generated by thermomechanical changes within the structure [17, 26, 27, 37, 38]. Therefore, it can be argued that a properly made weld should not modify the overall mechanical behavior of the material. In addition, standards for pipe manufacturing and joining impose that each time external parameters are changed, the alteration of the initial microstructure should be spared if not ameliorated for a better resistance and much safer service operations [38].

In the first place, the observed reproducibility of the stress–strain curves of the inner layers (WIL) is prominent for the test specimens having broken off the welding joint (Fig. 9a); however, dispersion increases and becomes

Fig. 6 Normalized dimensions for standard type IV welded specimen
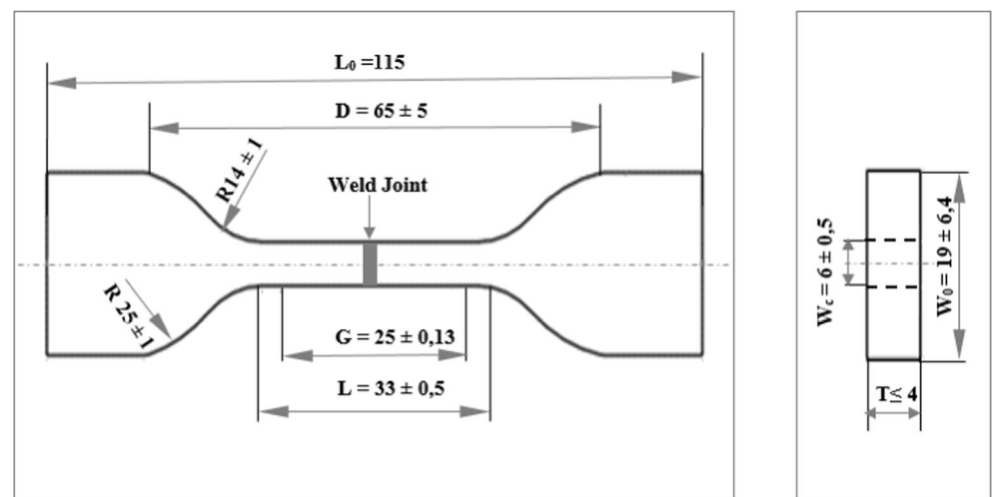
Fig. 7 **a** Pipe turning. **b** Pipe boring. **c** Extraction of standard test specimens out of inner (1. WIL), middle (2. WML), and outer (3. WOL) layers

a) Turning

b) Boring

c) Test specimen extraction
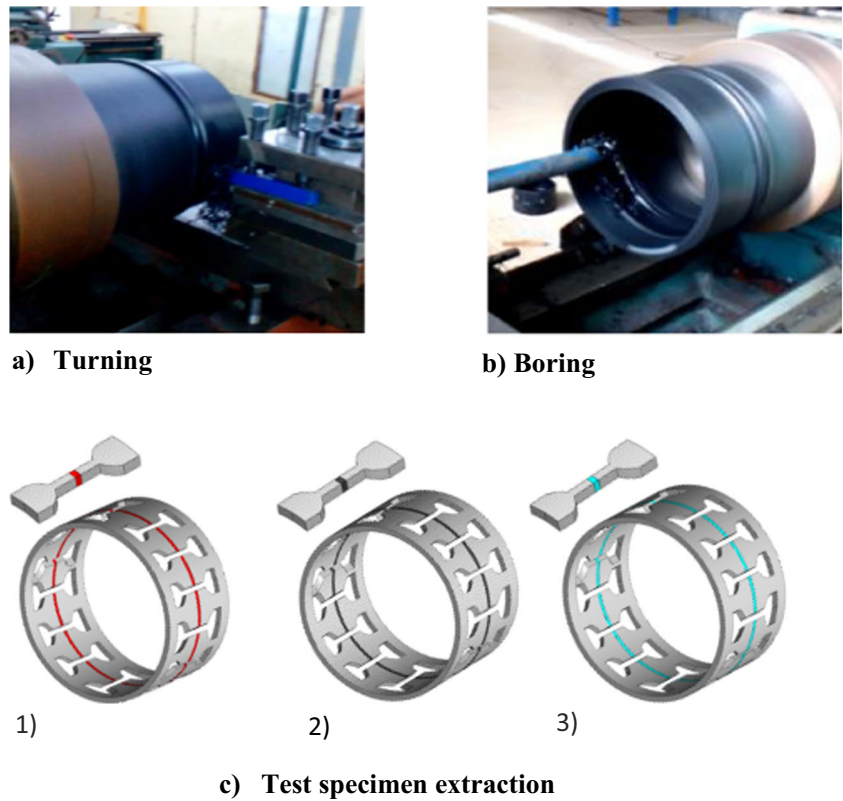
noticeable in zone III when moving in the radial direction of the pipe, i.e., from WIL towards WOL. Indeed, Fig. 9a–c indicates that the dispersion is initiated at different levels of deformations (300, 250, and 25%, respectively, for WIL, WML, and WOL). Also, the mechanical properties represented by σ_y, σ_f, and ε_f increased, which indicates a higher resistance and a better ductility of the outer welded layers (WOL) compared to WIL and WML despite the recorded differences. When considering the welded inner and outer layers, σ_y and σ_f increased by 19 and 22%, respectively, whereas the increase of the same properties among WIL and WML remains much lower, i.e., 12 and 6%, respectively. The resulting deformations at break (ε_f) showed little variation in the three cases, and they are spread out approximately between 425 and 600% with a slight importance for the WOL layers.

Throughout zone II, a small drop in the cold drawing stress is observed for each stress–strain curve of welded specimens as confirmed from literature [35]. This intrinsic instability corresponds to the moment when the neck passes through the weld causing a stress drop. Both size and shape are kept more or less invariant for all curves of the given layers (WIL, WML, and WOL). These events took place in the cold drawing zone at relatively specified intervals of fairly constant stresses (σ_{cd}). It should be noted that the occurrence intervals are functions of the position through the pipe wall. In terms of % deformations, these ranges are [28–95%], [105–160%],

and [160–230%], respectively, for WIL, WML, and WOL. When superimposing the three results, it becomes evident that these ranges encompass a continuous span of the cold drawing zone equivalent to more than one half (> 50%) of zone II (Table 5). The average stress level (σ_{cd}) increased as a function of layer position when going towards the outer layer (WIL ~ 14 MPa, WML ~ 15.5 MPa, and WOL ~ 17 MPa) (Fig. 9).

4.3 Comparison of unwelded and welded behaviors

Figure 10 compares each couple (unwelded and welded) stress–strain curves with the highest σ_y among the six cases considered in this study when the final failure took place outside the joint. For unwelded and welded sets, the identified tests are (UIL06, UML06, UOL01) and (WIL08, WML08, WOL07), respectively. The observed orders as a function of σ_y are as follows:

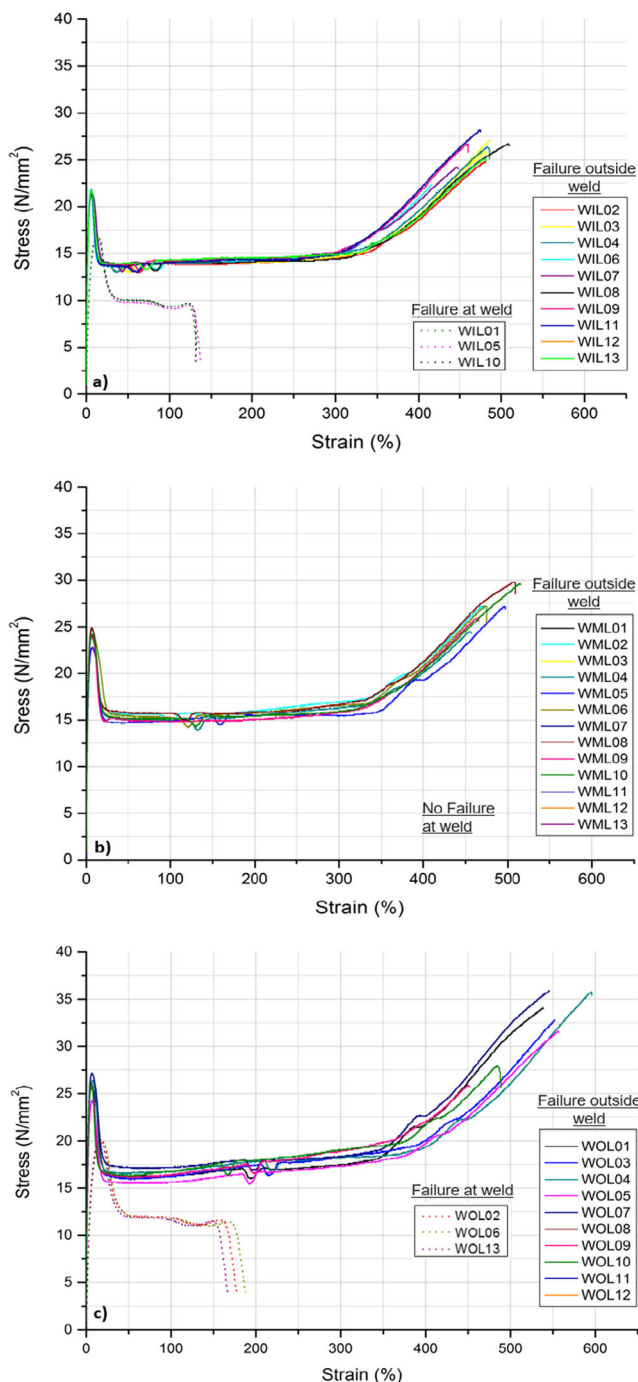$$\sigma_{y|UIL} > \sigma_{y|UML} > \sigma_{y|UOL} \tag{3}$$

$$\sigma_{y|WOL} > \sigma_{y|WML} > \sigma_{y|WIL} \tag{4}$$

It is noticed that the orders are inverted as the unwelded case indicates that the inner layer is the strongest; the higher crystallinity at the pipe inner surface usually enhances such strength [16, 21]. For the welded cases, melting, mixing, and
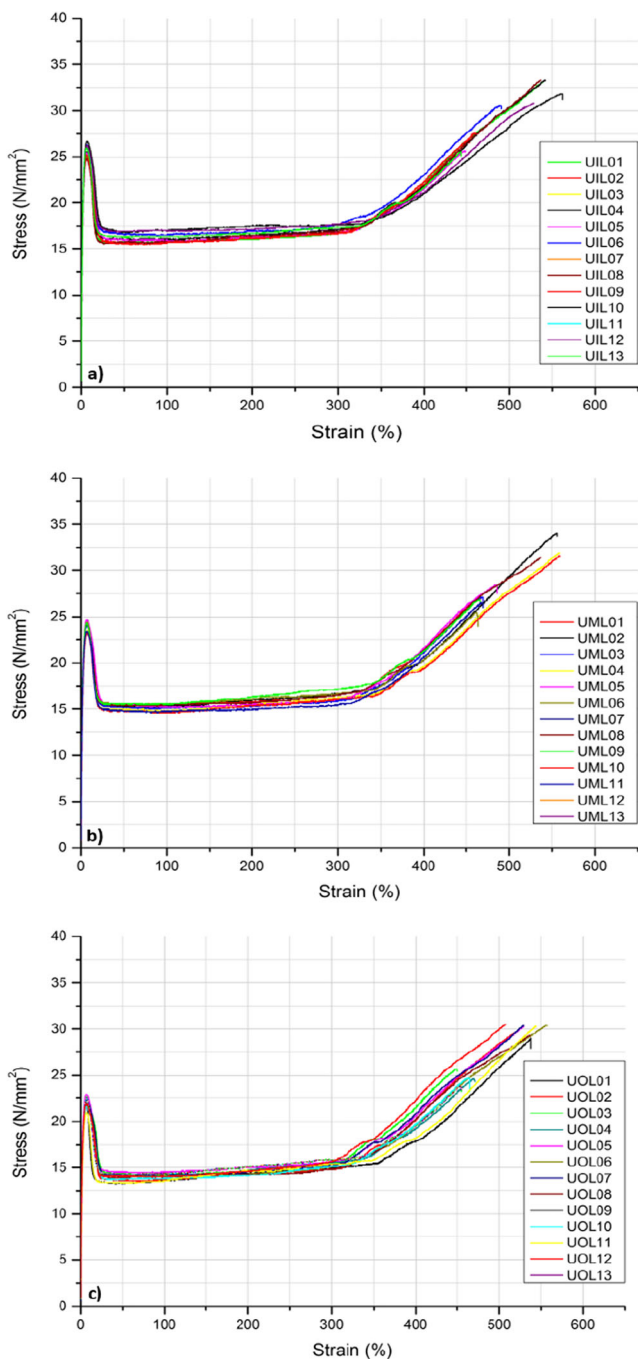
Fig. 8 Unwelded pipe σ–ε curves: **a** inner (UIL), **b** middle (UML), and **c** outer (UOL) layers

Fig. 9 Welded pipe σ–ε curves: **a** inner (WIL), **b** middle (WML), and **c** outer (WOL) layers

cooling operation offer a *new* mechanical behavior to the compound in addition to heat-affected zones around the weld and the indications (a), (b), and (c) shown in Fig. 10 point at the onset of weld material drawing [17, 29, 38]. In the same way, Fig. 11 compares stress–strain behavior with the highest σ_y when failure occurred at the weld (WIL08, WML08, WOL07) and out of the joint (WIL10 and WOL02). For instance, when the failure took place at the joint, σ_y for WOL02 dropped by 27% (reference WOL07) and ε_f for WIL10 jumped down by

more than 74% (reference WIL08). Compared to corresponding normal curves, brittle-like failure at the weld shows incredibly unacceptable results. Again, the order is respected for the welded case although the middle layer did not provide any failure at the weld (Inequality 5):

$$\sigma_{y|WOL}^{failure\ at\ weld} > \sigma_{y|WIL}^{failure\ at\ weld} \qquad (5)$$

Table 5 Comparison of <$\Delta\varepsilon_{cd}$>, <$\Delta\varepsilon_{weld\ streching}$>, % failures, and relative decreases of σ_y, ε_f, and σ_{cd} for the welded layers (WIL, WML, and WOL)

Characteristic	Symbol/unit	WIL	WML	WOL
Overall extent of drawing, zone II, Fig. 9 (failure off weld)	<$\Delta\varepsilon_{cd}$>, % strain	17–310	25–330	20–350
Corresponding strain interval for stress instability due to weld stretching, zone II, Fig. 9 (failure off weld)	<$\Delta\varepsilon_{weld\ streching}$>, % strain	28–95	105–160	160–230
Failures at weld	%	23.07	0 (No Failure)	23.07
Relative decrease of σ_{cd}, zone II, (failure off weld vs. at weld)	%	29.80	–	31.30
Relative decrease of σ_y zone II, (failure off weld vs. at weld)	%	22.83	–	25.92
Relative decrease of ε_f zone III, (failure off weld vs. at weld)	%	24.51	–	31.56

On the other hand, approaching properties in radial and circumferential directions made it possible to detect the weakest parts of the weld by reducing the cross-sectional area for mechanical characterization (i.e., instead of one test specimen, this method allowed the confection of three specimen lots as shown in Fig. 7). Therefore, a field weld which might be accepted after visual inspection may well reveal local substandard portion of the complete joint. In this study, it turned out that six test pieces belonging to WIL and WOL (three of each) have failed at the weld interfaces and show low elongation at break (Fig. 9). As expected, the mechanical characteristics are significantly reduced by almost a quarter for σ_y and by a third for ε_f. The cold drawing zone is also largely affected by the joint failure; the average value of σ_{cd} dropped by ~30% and evolved without ultimate plastic hardening. Finally, the middle layers (WML) remained firm and reliable as they did not show fracture at the welding joints, probably because the edges of the WML specimens were not affected by the formation of seam beads and that material fusion has proceeded correctly along the contact melting area (Fig. 11). On the other hand, brittle-like failures caused by incomplete fusion, dusty environment, and initial surface defect, for the cases WIL and WOL, are possible at both external and internal surfaces.

4.4 Mechanical property evolution

Figures 12, 13, 14, 15, 16, and 17 illustrate some typical mechanical properties of polyethylene for the three cases: (i) unwelded, (ii) failure at the weld, and (iii) failure outside the weld throughout the pipe wall layers (IL, ML, and OL). The analysis is made on the basis of a comparison between results at the three positions (inner, middle, and outer). The Young's modulus of the as-received material exhibits the following order (Fig. 12):

$$E_{unwelded}^{inner} > E_{unwelded}^{middle} > E_{unwelded}^{outer} \qquad (6)$$

When considering the welded case, the opposite order is observed; i.e., the maximum E is associated with WOL. These conclusions are identical for the yield stress (Fig. 13) and the nominal failure stress (Fig. 14). It should be mentioned that the properties resulting from weld joint failure are generally much lower (Figs. 12, 13, and 14). In terms of deformation at
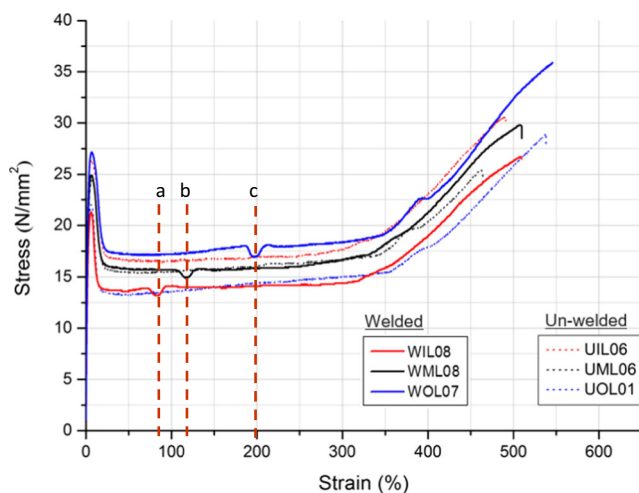

Fig. 10 Comparison between representative σ–ε curves for unwelded (UIL, UML, and UOL) and welded (WIL, WML, and WOL) specimens. Dotted lines "a," "b," and "c" show the onset of weld drawing
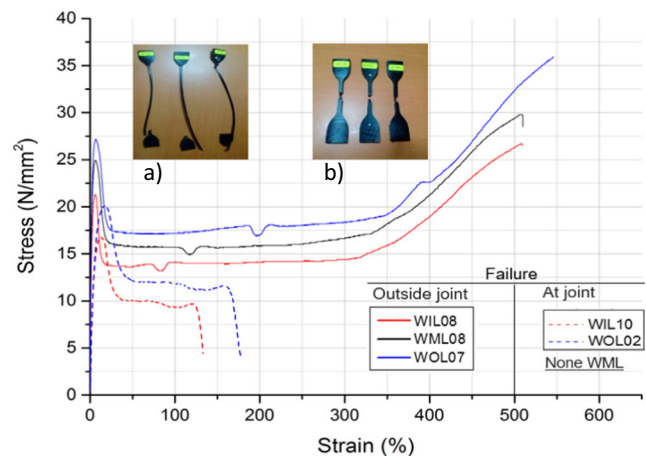
Fig. 11 Comparison between representative σ–ε curves for welded specimens with **a** highly ductile rupture outside the weld (WIL08, WML08, WOL07) (left picture) and **b** failure at the joint with reduced ductility (WL10, WOL02) (right picture). No weld failure observed for the middle layer (WML)

Fig. 12 Young's modulus
variation for different positions
across pipe wall
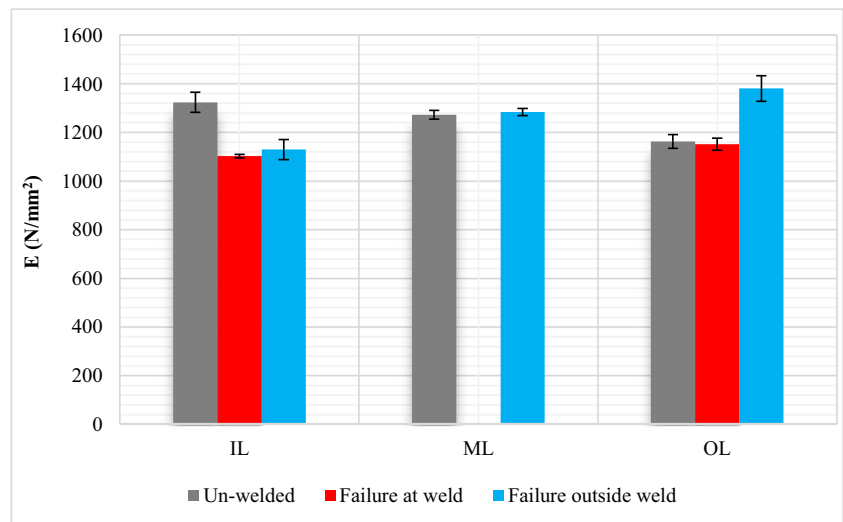
break, the three positions provided practically the same values for the unwelded case; however, the introduction of the weld disrupted such steadiness as ε_f dropped between 14 and 18% for inner and middle layers. On the outer layer, the deformation at break of the welded case remained comparable to the unwelded case while it decreased as much as 78% for failure occurring at the welding joint (Fig. 15). Usually, weld quality can be checked through ε_f, i.e., the closer the % elongation at break to that of unwelded material, the better it is [27, 35, 38]. In this study, such condition is validated particularly for WOL as the variation of average ε_f between unwelded and welded specimens is close to zero and it did not exceed 20% for both WIL and WML.

The other two important properties of semi-crystalline polyethylene which were analyzed are cold drawing stress level (σ_{cd}) and the extent of the drawing zone ($\Delta\varepsilon_{cd}$) [16, 20]. It is observed that the tendency for σ_{cd}, when going from inner to outer layers, is the same as for E, σ_y, and σ_f: (i)

decreasing for the unwelded cases and (ii) increasing for the welded cases no matter where the failure is occurring (Fig. 16). For $\Delta\varepsilon_{cd}$, the overall results show almost the same levels within less than 9% difference for unwelded and failure outside the weld specimens. It is concluded that this property is not affected by the presence of the weld; in other words, material drawing is mostly a function of the available amount of material to deform (Fig. 17). In Figs. 12, 13, 14, 15, 16, and 17, breaking at the weld yielded the lowest properties in terms of stresses and deformations in all layers.

4.5 Microstructure evolution

Available research literature, in connection with the present study, treated butt fusion welding in the framework of three complementary aspects: (i) mechanical properties associated with weld microstructure seeking descriptive details and explanatory arguments [35, 37, 38], (ii) search for novel and

Fig. 13 Yield stress variation for
different positions across pipe
wall
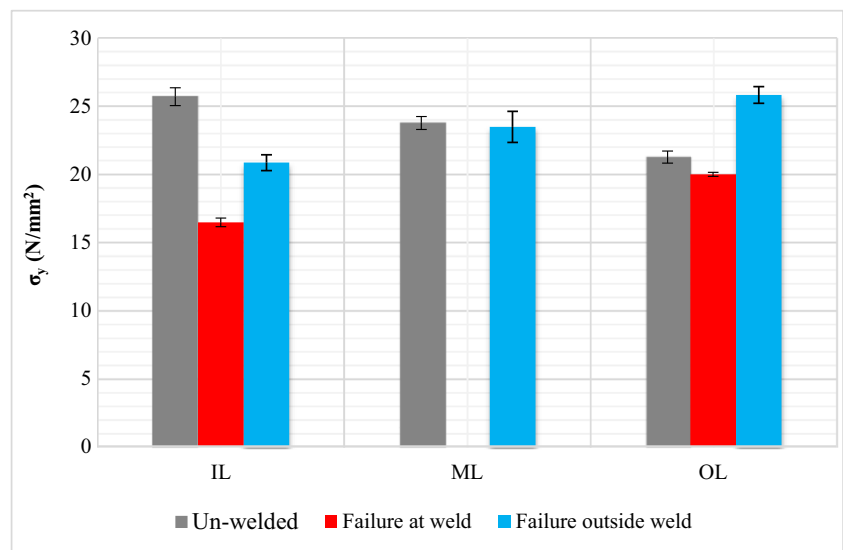
Fig. 14 Nominal failure stress variation for different positions across pipe wall
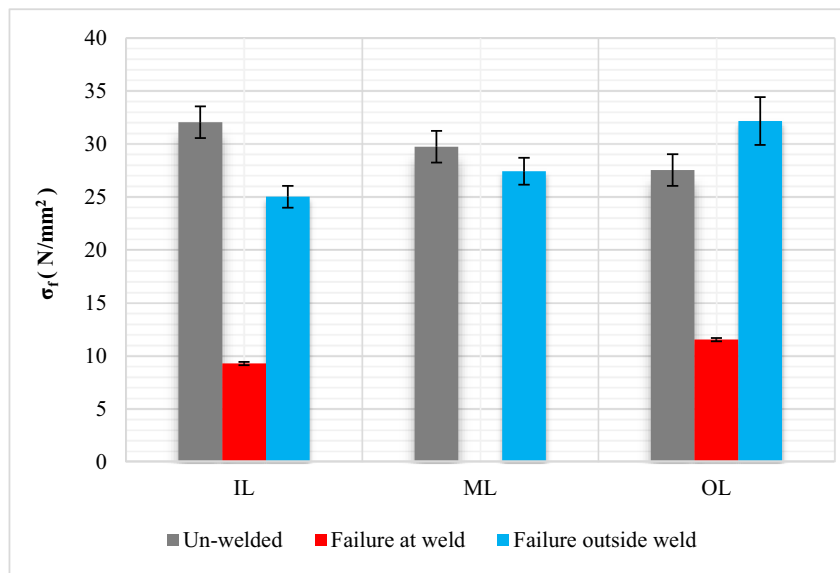

efficient characterization techniques (especially NDT methods) to analyze the melting zone and its phases [24–26, 29, 39], and finally (iii) weld quality, defect analysis, reliability, and long-term durability [40–43]. Although many authors have tried to establish correlations between structure and mechanical properties in semi-crystalline bulk PE, the underlying explanations are not well understood since pipe chemical composition is constantly ameliorated by co-polymerizations and new additives (stabilizers, antioxidants, pigments…) and under the pressure of industrials who keep on validating newly developed products for practical requirements such as double-walled pipes, corrugated pipes, and large-diameter plastic pipes [39].

For structure characterization, it has been established that the initial elastic deformation (zone I, Figs. 8 and 9) is a combination of lamellar separation, interlamellar shear, and lamellar stack rotation [38]. On the other hand, literature identifies a

lot of mechanisms of plastic deformation in zones II and III such as chain slip, lamella fragmentation and cavitation, deformation twining, and transverse slip [17, 38]. It is also advanced that during welding, two regions are competing at different scales: (i) a zone of thermal and gross rearrangement of structure and (ii) a zone of actual interdiffusion. In this study, it was observed that middle layers (UML and WML) have very similar mechanical properties related to stresses (E, σ_y, σ_f, and σ_{cd}). Similar ε_f values have been observed particularly for UOL and WOL, while those related to WML and UML are a little lower, but since all of them are > 400%, this is a good indication that they were performed at optimum conditions (Fig. 15). Usually, when the weld is carried out correctly, failure occurs through fibrillation (highly yielded fibrils), and our findings are in agreement with literature results especially for σ_y and ε_f [17, 29, 35, 38].

Fig. 15 Failure strain variation for different positions across pipe wall
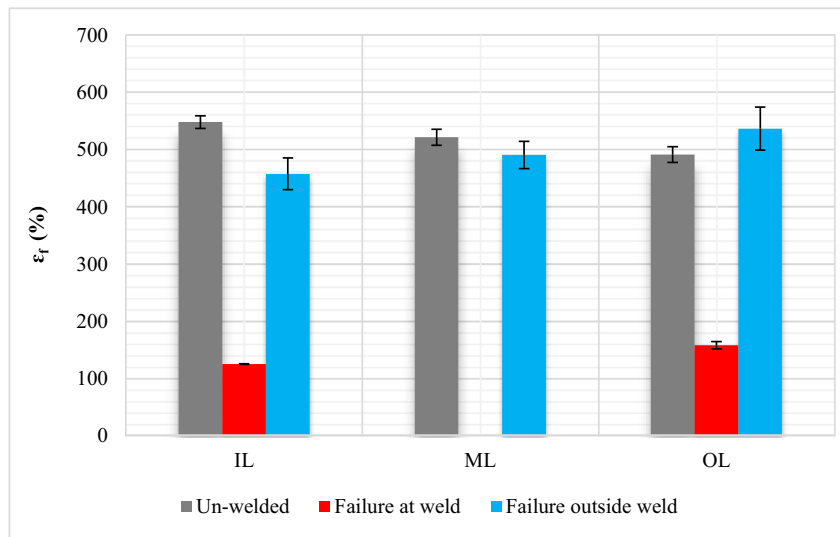
Fig. 16 Cold drawing stress variation for different positions across pipe wall
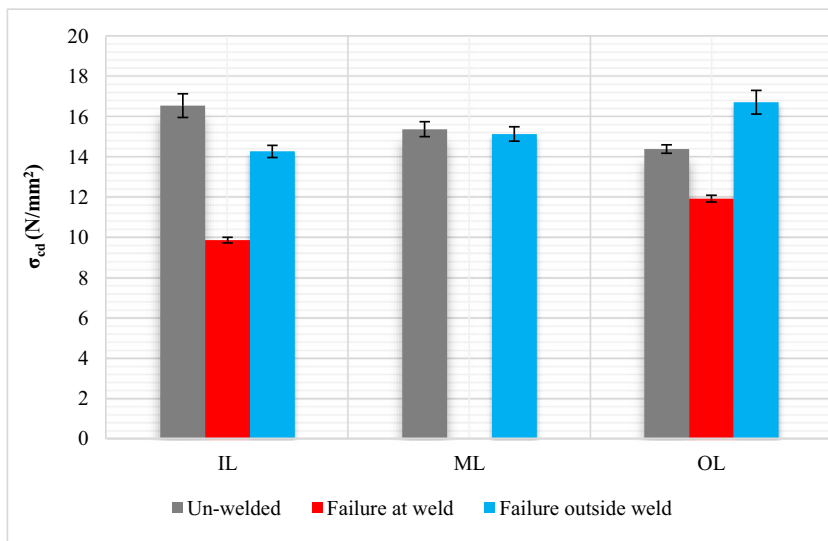

Weld mechanical properties are also functions of the conditions in which welding was performed as any overdesigned dwell time (Table 2) may influence poorly both stress and strain parameters [17]. When studying the micromechanical properties across butt fusion welds using microindentation (MI) technique, it is revealed that the melt zone (MZ) is surrounded by a heat-affected zone (HAZ) characterized by an ongoing rise in material properties in comparison to parent material [29]. In addition, MI conclusions allowed drawing the HAZ boundaries and put in evidence annealing as the main cause of micromechanical property amelioration. It was also observed that the size of the MZ is the smallest at the pipe wall midpoint and widens gradually as it gets to outer and to inner borders (Fig. 2) [12, 29, 34]. As a result, this finding is in correlation with our study in order to explain

superior performance of WML specimens (0% failure at weld) compared to both WIL and WOL ones where 23% failure was observed at the weld (Table 5). Alternatively, it is established that microstructural changes in the HAZ start with a thin and fine spherulitic zone which is formed due to rapid cooling followed by a columnar zone (or lamellar-type structure) and finally comes the deformed zone (often called shear melt zone) having relatively coarse spherulites. One way to explain differences between properties shown in Figs. 12, 13, and 14 could be the presence of coarse spherulite boundaries which are the most probable trajectories followed by brittle failure [40].

Table 6 summarizes welding conditions and results of several studies that have examined the evolution of polyethylene pipe microstructure [13, 17, 26–29, 38]. The welded zone

Fig. 17 Extent of cold drawing variation for different positions across pipe wall
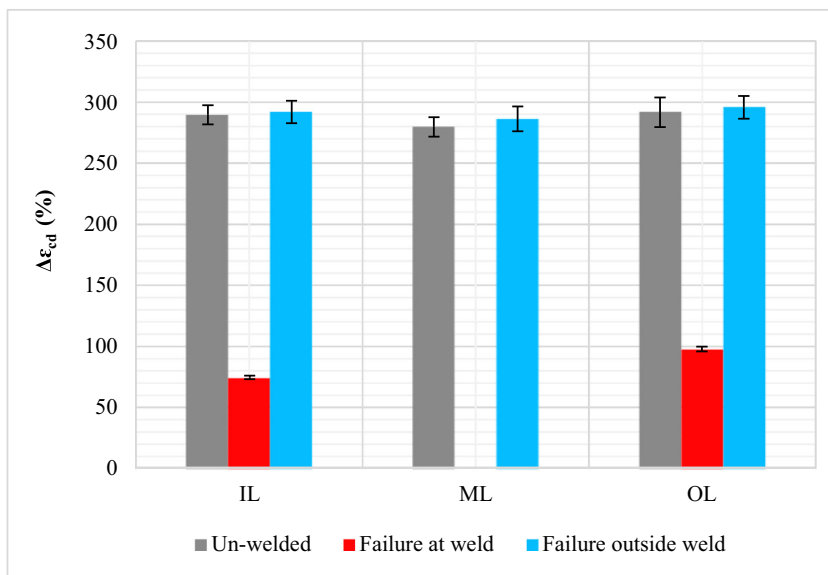
Table 6 Comparison of crystallinity measurements for unwelded and butt fusion welded PE pipes

Reference	Conditions	Position/method	% Crystallinity	
			Unwelded	Welded
Hogbin and Peng [28]	HDPE-100, OD 200 mm; t 11.9 mm (SDR 17), $T°$ 220 °C, and $P°$ 0.2 MPa	XRD	66.78	69.50
Shaheer et al. [29]	HDPE-100, OD 180 mm; t 16.4 mm (SDR 11), $T°$ 230 °C; $P°$ 0.15 MPa		63.8	67.8
Talhi et al. [13]	MDPE-80 (Y-PE, OD 90 mm; SDR 11 (t_{min} 8.2 mm, from BS-ISO-4427); welding at $T°$ 210 °C; $P°$ 0.15 MPa	IL	45.4	44.8
		ML	45.0	45.7
		OL	42.6	46.0
Pashupati et al. [17]	HDPE pipe, OD 110 mm; SDR 9 (t_{min} 12.3 mm, from BS-ISO-4427); $T°$ 231 °C; $P°$ 0.41 MPa (changing welding times to simulate cold defects)		51.50	57.10
Galchun et al. [26]	Welding of dissimilar HDPE pipes (PE-80 and PE-100); OD 63 mm, t 6 mm; $T°$ 200 °C and $P°$ 0.2 MPa	DSC PE-80	42	53 (PE Mix)
		DSC PE-100	51	
		WAXS PE-80	56	66 (PE Mix)
		WAXS PE-100	57	
Hehn [27]	HDPE-100 (TU B121); OD 160 mm; t 14.6 mm (SDR 11); $T°$ 220 °C; $P°$ 0.18 MPa	IL	74.1	74.2
		ML	73.8	73.4
		OL	70.1	74.3
Leskovics et al. [38]	HDPE-80, Hexene-1 co-monomer, OD 160 mm, t 9.8 mm; $T°$ 190 °C; $P°$ 0.15 MPa	DSC	49.5	55.1
		XRD	52	55
Niou et al. (this study)	HDPE-100; OD 200 mm; t 11.9 mm (SDR 17); $T°$ 220 °C; $P°$ 0.18 MPa (see Tables 2, 3, and 4)	IL	53.91	49.38
		ML	51.03	51.45
		OL	49.11	58.34

material undergoes many transformations such as melting, deformation, and molecular interpenetration, and then followed by recrystallization, i.e., formation of new structure under the imposed stress state of the welding process [38]. Consequently, microstructures of the weld interface and its heat-affected zones establish the ultimate mechanical properties of the joint [40]. In other words, both heating and cooling processes at the weld creates microstructures that differ from unwelded material. In principle, mechanical properties and interfacial strength of the joint are affected by the thickness of the MZ as thin ones give the weld brittleness and lower the strength whereas higher MZ thickness and wider HAZ increase the weld strength. In addition, residual stresses are usually caused by the non-homogeneity of flow and temperature gradients during welding. Such findings led to distinguish five zones in weld microstructure by which are (i) skin remnant; (ii) spherulitic, slightly elongated; (iii) columnar; (iv) boundary nucleation; and (v) spherulitic [34, 44]. The last zone made of spherulites has been recognized as the basic morphology of semi-crystalline polymers.

Usually, the degree of crystallinity is the first structural parameter that has been correlated to mechanical properties at different zones of butt fusion joint [44]. During welding, the process that pipes undergo from fusion temperature to room temperature is the same as an annealing process. So, the more high anneal temperature is, the more high crystallinity degree of polymer is, which "explains crystallinity evolution throughout the pipe wall" [45]. Crystallinity comparisons are principally made on welded and unwelded pipes using the DSC method and sometimes the XRD method. Two types of comparisons are reported according to the location of the measurement of crystallinity. In other words, either the crystallinity is measured globally or by considering localized sampling positions in the wall following the three previously delimited layers (IL, ML, and OL) (Table 4 and Fig. 2). Since the welding conditions are dictated by the standards and the manufacturers' recommendations, they are supposed to provide more resistant joints compared to the original material. For the overall sampling measurements, it is found that crystallinity increases for the welded material as the differences are within the interval 3 to 10%. Therefore, it can be stated as a general rule:

$$\chi_{welded} > \chi_{unwelded} \tag{7}$$

For that reason, it is reasonable to observe higher mechanical properties for welded cases as it was discussed for E, σ_y, and σ_f (Figs. 12, 13, and 14). The same argument can be invoked for the cold drawing stress (σ_{cd}, Fig. 16). The measurements made according to this proposed method using the three layers (IL, ML, and OL) are in conformity with those of

the literature, and it is concluded that there is an evolution of crystallinity throughout the pipe wall for welded (Eq. 8) and unwelded (Eq. 9) cases as follows:

$$\chi_{welded}^{inner} < \chi_{welded}^{middle} < \chi_{welded}^{outer} \tag{8}$$

$$\chi_{unwelded}^{inner} > \chi_{unwelded}^{middle} > \chi_{unwelded}^{outer} \tag{9}$$

These results indicate that the effect of the supplied heat and the material melting contributed in creating a more ordered structure as deduced from crystallinity data. By performing the proposed localized analysis, it is found that the outer layer (OL) always follows the same trend as in inequalities (8) and (9). Indeed, the crystallinity in our case increased by 15% as confirmed by other studies for the OL layer [13, 38]. For the intermediate layer (ML), the results found indicate very little change in the crystallinity between the welded and unwelded specimens with a difference < 1%. This is in agreement with results of other studies of the literature on crystallinity [13, 27]. This might have a relation with the position of this layer which is protected by the other two layers and thus limiting the effects of external disturbances in terms of unwanted material cooling or heat loss by natural convection. Although the interface is made of molten material from both pipe ends, chain entanglements and cooling are achieved under conditions similar to extrusion, and thus, the final structure would be at a similar level of crystallinity [13, 27]. Lastly, crystallinity measurements for the inner layer (IL) are in favor of the welded pipes compared to unwelded ones; however, some studies did not find significant variations, and they generally remain below 1% [27]. This conclusion can be extended even to the welding of pipes of dissimilar resins (HDPE-100 and HDPE-80) where it has been found that crystallinity is improved up to 20% for welded cases as shown in Table 6 [26]. Also, globally, crystallinity results show variations within the range 3 to 20%, whereas for the localized measurements, the % changes are smaller especially for the inner layers (1 to 7%). For the middle layer where the weld quality is found to be the highest as no failure was observed for this lot, crystallinity measurements are less dispersed and the percent change remained below 1%. On the other hand, for the outer layers, the differences ranged from 5 up to 15%.

Figure 18 illustrates the results obtained in this study. An increase in crystallinity is observed for welded pipes from inner to outer layers, while for unwelded ones, the evolution is in opposite direction. Such situation is confirmed by the literature data as discussed previously for Table 6. In addition, for the base pipe (unwelded), the evolution is also confirmed by other studies for two different pipe resins (HDPE-80 and HDPE-100) [22, 23]. The study of crystallinity in welded and

Fig. 18 Crystallinity evolution for unwelded and welded pipes as a function of wall position
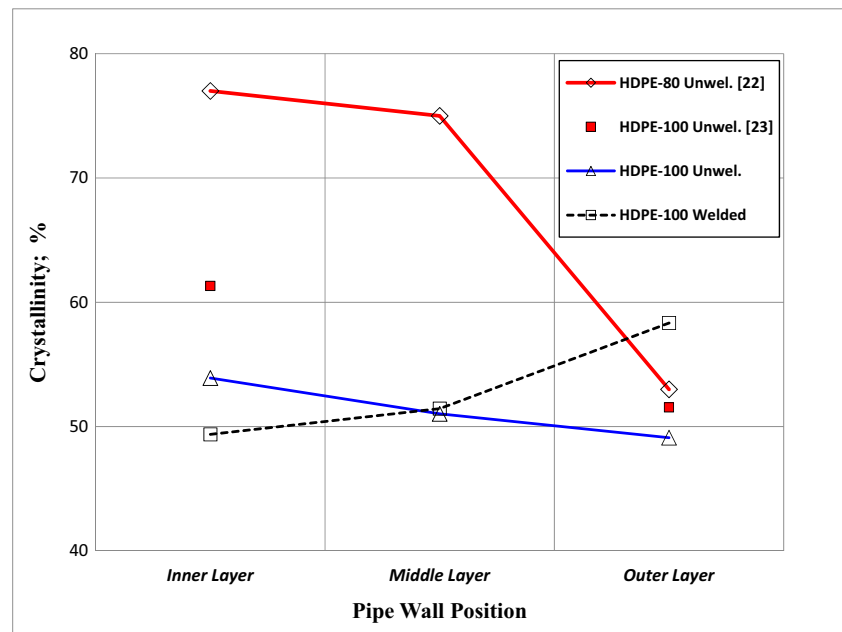
unwelded pipes has established that the presence of a weld gives better mechanical strength, and if a fracture will take place, the probability that it will occur at the weld is very low given the crystalline structure which settled down. Therefore, the observed failures at the weld in Fig. 9 and whose rate reached 23% (likewise WIL and WOL, Table 5) are a good indication that this method is capable of providing information and detecting localized defects usually unnoticed during global testing. Furthermore, this method could be used to verify the adequacy between welding parameters (Table 2) and newly fabricated polyethylene resins to discern possible localized weld weaknesses.

Weld quality faces many challenges such as welding different HDPE resins or the new double walled HDPE pipes designed for specific fluid transport. For instance, when manufacturing joints involving PE-80 and PE-100, which is a real situation in today's network functioning (repairs or new extensions), it is revealed that reorganization of crystalline phases occurs and crystalline areas with higher mechanical and thermal properties appear due to the increase of crystallite quantity, their bigger size, and the better crystallite packing [39]. For irregular joining area topology, likewise double-walled pipes, butt fusion welding technique can be also employed successfully. Microscopic weld investigation confirmed a uniform melt area without defects and a complete interface fusion which prevented the reduction of the mechanical performance [26]. These examples emphasize the increasing technical difficulties in studying the weld zone in future possible new designs. The existing characterization methods are adapted and improved whenever possible, but the objectives usually stay unchanged in terms of best

mechanical properties, homogenous microstructure, and reliable welding techniques.

5 Conclusion

This investigation is designed to set up a method in order to evaluate the intrinsic localized resistance of HDPE pipes. The method compares stress–strain behaviors of welded and unwelded pipes. Test specimens are extracted from machined pipe portions along the circumference for varied thicknesses.

The main conclusions which can be drawn from this research work are

1. An experimental method is established to study localized stress–strain behaviors based on standard mechanical tests. It consists of five simultaneous steps: (i) pipe preparation based on SDR, (ii) pipe butt fusion welding, (iii) combined turning and boring machining at specified conditions, (iv) standard specimens cutting, and (v) mechanical testing.

2. The method is successfully applied for welded and unwelded 200-mm OD pipe. The most important result is the 23% failure at weld for WIL and WOL, while no weld breakdown was observed at any WML-localized positions. This indicates that the most vulnerable parts are those being rapidly cooled by ambient air (cold weld phenomenon). Such problem cannot be detected when testing the whole pipe thickness.

3. The three characteristic zones of stress–strain behavior in semi-crystalline materials are preserved even in the

presence of a butt fusion weld. The effects of weld on the mechanical properties have been evaluated. At the inner layers (WIL), the properties E, σ_y, σ_f, and σ_{cd} displayed notably lower values, whereas in the outer layers (WOL), the tendency is inversed.

4. The values of $\Delta\varepsilon_{cd}$ remain approximately steady for unwelded and welded cases across the pipe wall. It can be concluded that this property is less affected by the presence of the weld since it describes a constant flow of material and is mostly a function of material quantity available for cold drawing.

5. Microstructure analysis shows that welding contributed to crystallinity increase giving higher strength to the joint. When applying the proposed method, it is found that crystallinity decreased for unwelded pipe from inner to outer layers and the inverse is observed for the welded case. Such reorganization of structure crystallites explains the mechanical properties tendencies.

6. Whenever failure occurs at the weld, all properties resulting from stress–strain behavior show a net regression. Consequently, the approach developed here gives consistent indications on welding quality and goes further by allowing access to the different segments of the various layers of a pipe. Moreover, the outermost and innermost welded layers may exhibit lower or yet bad-quality welds as imperfections can concentrate stresses at the joint interface and allow crack initiation. It can be advanced that the presence of coarse spherulite boundaries in the HAZ is a probable trajectory which can be followed by brittle-like failure when occurring at the weld.

7. This method is an attractive example when compared to the microindentation technique as both approaches help extract complementary information and may validate each other. For instance, elastic modulus data issued by the two techniques are in good agreement, but the MI technique allows defining the contour of both MZ and HAZ. On the other hand, "localized" mechanical testing gives prompt information for quality control and provides other methods with needed validation data.

Nomenclature a_p, Depth of cut (mm); E, Elasticity modulus (MPa); f, Feed rate (mm/rev); G, Gage length (mm); ID, Inner diameter (mm); L, Narrow section length (mm); L_0, Overall specimen length (mm); OD,

Outside diameter (mm); $P°$, Welding pressure (MPa); R_i, Inner radius (mm); R_o, Outer radius (mm); t, Pipe thickness (mm); $T°$, Welding temperature (°C); V_c, Cutting speed (m/min); W_c, Narrow section width (mm); w_o, Overall width (mm)

Greek letters $\Delta\varepsilon_{cd}$, Extent cold drawing strain (%); ε_f, Failure strain (%); σ_{cd}, Cold drawing stress (MPa); σ_f, Nominal failure stress (MPa); σ_y, Yield stress (MPa); χ, Crystallinity (%)

Abbreviations   BFW, Butt fusion weld; HAZ, Heat-affected zone; HDPE, High-density polyethylene; MDPE, Medium-density polyethylene; MI, Microindentation; MZ, Melt zone; NDT, Non-destructive testing; PE, Polyethylene; SDR, Standard dimensions ratio; UIL, Unwelded inner layer; UML, Unwelded middle layer; UOL, Unwelded outer layer; WIL, Welded inner layer; WML, Welded middle layer; WOL, Welded outer layer

References

1. Wilson D, Filion Y, Moore I (2015) State-of-the-art review of water pipe failure prediction models and applicability to large-diameter mains. Urban Water J 14(2):173–184. https://doi.org/10.1080/1573062X.2015.1080848

2. Yu K, Morozov EV, Ashraf MA, Shankar K (2017) A review of the design and analysis of reinforced thermoplastic pipes for offshore applications. J Reinf Plast Compos. https://doi.org/10.1177/0731684417713666

3. Deblieck RAC, van Beek DJM, McCarthy M, Mindermann P, Remerie K, Langer B, Grellmann W (2017) A simple intrinsic measure for rapid crack propagation in bimodal polyethylene pipe grades validated by elastic–plastic fracture mechanics analysis of data from instrumented Charpy impact test. Polym Eng Sci 57:13–21. https://doi.org/10.1002/pen.24380

4. Sharma GVSS, Umamaheswara Rao R, Srinivasa Rao PS (2017) A Taguchi approach on optimal process control parameters for HDPE pipe extrusion process. J Ind Eng Int 13(2):215–228. https://doi.org/10.1007/s40092-016-0179-1

5. Han L-H, Deng Y-H, Liu C-D (1999) The determination of JIC for polyethylene pipe using non-standard arc-shaped specimen. Int J Press Vessel Pip 76:647–651. https://doi.org/10.1016/S0308-0161(99)00032-0

6. van der Stok EJW, Scholten FL (2016) Determining the residual quality of PE pipes using the strain hardening test. Proc. of the 18th plastic pipes Conf. PPXVIII, September 12–14, 2016, Berlin, 10p. https://doi.org/10.1134/S0021894417020183

7. Cherif MND, Elmeguenni M, Benguediab M (2017) Impact fracture toughness evaluation for high density polyethylene materials. J Appl Mech Tech Phys 58(2):335–341

8. Akkurt A (2014) An analysis of electro-melting and hot element welding methods' safety used to join PE natural gas pipes. Int J Mech Mechatron Eng 3(2):493–504

9. Saharudin MS, Atif R, Shyha I, Inam F (2016) The degradation of mechanical properties in polymer nano-composites exposed to liquid media (a review). RSC Adv 6:1076–1089. https://doi.org/10.1039/C5RA22620A

10. Hamlaoui N, Azzouz S, Chaoui K, Azari Z, Yallese MA (2017) Machining of tough polyethylene pipe material: surface roughness and cutting temperature optimization. Int J Adv Manuf Technol 92: 2231–2245. https://doi.org/10.1007/s00170-017-0275-4

11. Belhadi S, Kaddeche M, Chaoui K, Yallese MA (2016) Machining optimization of high density polyethylene pipe using the Taguchi method and grey relational analysis. Int Polym Process 31(4):491–502. https://doi.org/10.3139/217.3271

12. Guo S-M, Yang Z-G, Tang X-Y, Zuo Y-T (2017) Safety assessment of high density polyethylene pipe with thermal damages. J. Plast Rubber Compos Macromol Eng 46(4):1743–2898. https://doi.org/10.1080/14658011.2017.1301339

13. Talhi FZ, Benaniba MT, Belhaneche-Bensemra N, Massardier V (2016) Comparison of material properties in butt welds of used and unused polyethylene pipes for natural gas distribution. J Polym Eng 37(3):279–285. https://doi.org/10.1515/polyeng-2016-0015

14. Mikula J, Hutař P, Nezbedová E, Lach R, Arbeiter F, Ševčík M, Pinter G, Grellmann W, Náhlíka L (2015) On crack propagation in the welded polyolefin pipes with and without the presence of weld beads. Mater Des 87:95–104. https://doi.org/10.1016/j.matdes.2015.07.131

15. Vigier G, Degoulet C, Germain Y (2001) Physical and mechanical properties of polyethylene for pipes in relation to molecular architecture: I microstructure and crystallisation kinetics. Polymer 42:8425–8434

16. Kiass N, Khelif R, Boulanouar L, Chaoui K (2004) Experimental approach to mechanical property variability through a high-density polyethylene gas pipe wall. J Appl Polym Sci 97:272–281. https://doi.org/10.1002/app.21713

17. Pokharel P, Kim Y, Choi S (2016) Microstructure and mechanical properties of the butt joint in high density polyethylene pipe. Int J Polym Sci, Art. ID 6483295. https://doi.org/10.1155/2016/6483295. 13p

18. Jagtap TU, Mandave HA (2015) Machining of plastics: a review. Int J Eng Res Gen Sci 3((2) (Part 2)):577–581

19. Alauddin M, Choudhury IA, Baradie MAE, Hashmi MSJ (1995) Plastics and their machining: a review. J Mater Process Technol 54:40–46. https://doi.org/10.1016/0924-0136(95)01917-

20. Rehab-Bekkouche S, Ghabeche W, Kaddeche M, Kiass N, Chaoui K (2009) Mechanical behaviour of machined polyethylene filaments subjected to aggressive chemical environments. Mechanika (MECHANICS) 77(3):40–46

21. Alimi L, Ghabeche W, Chaoui W, Chaoui K (2012) Étude des propriétés mécaniques à travers la paroi d'un tube HDPE-80 extrudé destiné à la distribution du gaz naturel. Matér Tech 100(1):79–86. https://doi.org/10.1051/mattech/2012004 www.mattech-journal.org

22. Alimi L, Chaoui K, Ghabeche W, Chaoui W (2013) Short−term HDPE pipe degradation upon exposure to aggressive environments. Mater Tech 101:701. https://doi.org/10.1051/mattech/2013083 www.mattech-journal.org

23. Ghabeche W, Alimi L, Chaoui K (2015) Degradation of plastic pipe surfaces in contact with an aggressive acidic environment. 30. Int. Conf. Technol. & Mater. for Renew. Energy, Envir. & Sustainability. Energy Procedia 74:351–364. https://doi.org/10.1016/j.egypro.2015.07.625

24. Kafieh R, Lotfi T, Amirfattahi R (2011) Automatic detection of defects on polyethylene pipe welding using thermal infrared imaging. Infrared Phys Technol 54(4):317–325

25. Gueugnaut D, Tessier M, Bouaffre R, Lopitaux A (2017) Ultrasonic phased array inspection of electrofused joints implemented in polyethylene gas piping systems. J Mater Sci Eng A 7(3–4):68–81. https://doi.org/10.17265/2161-6213/2017.3-4.002

26. Galchun A, Korab N, Kondratenko V, Demchenko V, Shadrin A, Anistratenko V, Iurzhenko M (2015) Nanostructurization and thermal properties of polyethylenes' welds. Nanoscale Res Lett 10:138. https://doi.org/10.1186/s11671-015-0832-4 Springer Open Access, 6p

27. Hehn O (2006) Analyse expérimentale et simulation thermomécanique du soudage bout à bout de tubes de polyéthylène. PhD Thesis, Ecole des Mines de Paris, 20p

28. Dai H, Peng J (2017) The effects of welded joint characteristics on its properties in HDPE thermal fusion welding. Mod Phys Lett B 31(15):1750185:1–11. https://doi.org/10.1142/S0217984917501858

29. Shaheer M, Troughton M, Khamsechnezad A, Song J (2017) A study of the micro-mechanical properties of butt fusion-welded joints in HDPE pipes using the nano-indentation technique. Weld World 61:819–831. https://doi.org/10.1007/s40194-017-0454-9

30. BS ISO 4427–2 2007 British standard, Plastic piping system— polyethylene (PE) pipes and fittings for water supply—part 2: pipes; www.spic.ir

31. ASTM Standard D 638–02a 2002 Standard test method for tensile properties of plastics (metric), Annual Book of ASTM Standards

32. http://www.groupe-chiali.com/images/documentations/manuels_de_pose/man_bout_à_bout. Accessed Sept. 10 2017

33. ISO 12176–3 (2003) Plastics pipes and fittings—equipment for fusion jointing polyethylene systems—part 1: Butt fusion

34. Barber P, Atkinson JR (1974) The use of tensile tests to determine the optimum conditions for butt fusion welding certain grades of polyethylene, polybutene-I and polypropylene pipes. J Mater Sci 9:1456–1466

35. de Courcy DR, Atkinson JR (1977) The use of tensile tests to determine the optimum conditions for butt welding polyethylene pipes of different melt flow index. J Mater Sci 12(8):1535–1551

36. Kaddeche M, Chaoui K, Yallese MA (2012) Cutting parameters effects on the machining of two high density polyethylene pipes resins. Mech Ind 13:307–316. https://doi.org/10.1051/meca/2012029 www.mechanics-industry.org

37. Niou S, Azzouz S, Chaoui K, Azari Z (2016) Développement d'une méthode pour caractériser la résistance mécanique circonférentielle d'un joint de tube plastique soudé bout-à-bout, 10èmes Journées de Mécanique (JM'10, EMP), Ecole Militaire Polytechnique, 12-13 April, Algiers, 1–5

38. Leskovics K, Kollár M, Bárczy P (2006) A study of structure and mechanical properties of welded joints in polyethylene pipes. Mater Sci Eng A 419:138–143. https://doi.org/10.1016/j.msea.2005.12.019

39. Lee B-Y, Kim J-S, Lee S-Y, Kim YK (2012) Butt-welding technology for double walled polyethylene pipe. Mater Des 35:626–632

40. Tariq F, Nausheen Naz N, Khan MA, Baloch RA (2012) Failure analysis of high density polyethylene butt weld joint. J Fail Anal Prev 12:168–180. https://doi.org/10.1007/s11668-011-9536-y

41. El-Bagory TMAA, Younan MYA, Sallam HEM (2013) Mechanical behavior of welded and un-welded polyethylene pipe materials, K-PVP Conference, Proc. of the ASME, Pressure Vessel & Piping Division, Paper # 2013–97743, Paris, (14–18/07/13)

42. Lai HS, Kil SH, Yoon KB (2015) Effects of defect size on failure of butt fusion welded MDPE pipe under tension. J Mech Sci Technol 29(5):1973–1980. https://doi.org/10.1007/s1226-015-0418-1

43. Zhao JQ, Daigle L, Beaulieu D (2002) Effect of joint contamination on the quality of butt-fused HDPE pipe joints. Can J Civ Eng 29(5):787–798. https://doi.org/10.1139/l02-078

44. Atkinson JR, Barber P (1972) Some microstructural features of the welds in butt-welded polyethylene and polybutene-1 pipes. J Mater Sci 7:1131–1136

45. Qi F, Huo L, Zhang Y, Jing H (2004) Study on fracture properties of high-density polyethylene (HDPE) pipe. Key Eng Mater 261-263:153–158. https://doi.org/10.4028/www.scientific.net/KEM.261-263.153